

# Monopole-Antimonopole Correlation Functions in 4D $U(1)$ Gauge Theory

Luca Tagliacozzo\*

*Departament d' Estructura i Constituents de la Matèria,  
Universitat de Barcelona,  
647, Diagonal, 08028 Barcelona, Spain.*

We study the two-point correlator of a modified Confined-Coulomb transition order parameter in four dimensional compact  $U(1)$  lattice gauge theory with Wilson action. Its long distance behavior in the confined phase turns out to be governed by a single particle decay. The mass of this particle is computed and found to be in agreement with previous calculations of the  $0^{++}$  gaugeball mass. Remarkably, our order parameter allows to extract a good signal to noise ratio for masses with low statistics. The results we present provide a numerical check of a theorem about the structure of the Hilbert space describing the confined phase of four dimensional compact  $U(1)$  lattice gauge theories.

## INTRODUCTION

Quantum Chromo-Dynamics (QCD), the present theory for strong interaction, is formulated in terms of quark and gluon fields. The latter are carriers of the  $SU(3)$  symmetric colour interaction. At low energies, however, the only existing particles are hadrons. To explain this fact, one has to suppose that quarks are confined inside hadrons. The attempt to understand this obscure property of quarks, confinement, has led to study simplified models, defined on a lattice, but still exhibiting confinement [1]. The simplest among such models are Ising systems on two and three dimensional lattices. They possess global discrete symmetries. Their generalisation to local symmetries are known as gauge Ising models and still exhibit confinement [2, 3]. A further step to approach QCD is to consider models with continuous gauge symmetry in four dimensions (4D).

Among them is compact  $U(1)$  lattice gauge theory ( $U(1)$ lgt) [4]. This model has two phases: a confined phase at strong coupling and a Coulomb phase at weak coupling. The order and the location of the phase transition that separate them depend on the action form and has been a long standing subject of debate [5, 6, 7, 8]. The idea that monopoles could play a crucial role in the description of confinement appeared after the inspiring work of Polyakov [9] in three dimensions and the contemporary conjecture, known as dual superconductivity (DS), by Mandelstam and 't Hooft about confinement in QCD [10, 11]. This conjecture states that confinement could be described by a mechanism similar to that responsible of superconductivity. In the confined phase, the vacuum should be filled with monopoles in the same way a superconductor ground state is filled with Cooper pairs. In the case of  $U(1)$ lgt a finite density of monopoles was discovered in the confined phase and vanishing in Coulomb phase [12].

The introduction of a well defined order parameter for the Confined - Coulomb transition in  $U(1)$ lgt [13, 14, 15, 16] proved, eventually, the condensation of monopoles at the transition. Using the Wilson action, this transition can be shown to be of first order (with very long correlation length) and located, in the thermodynamic limit, at  $\beta_c \approx 1.011$  (for recent high precision measurements of the transition point see [7]). It is this order parameter, a monopole creation operator, that allows to rigorously distinguish between the Confined and the Coulomb phases of  $U(1)$ lgt. Other equivalent order parameters have been constructed later [8].

In [16], a preliminary study of the mass of the monopole had allowed to claim that the DS exhibited in the Confined phase of  $U(1)$ lgt was of type II. In [17], a similar study has been attempted with the Villain action but the authors could not gain enough statistics to study the monopole mass in the confined phase.

After the work of Seiberg and Witten [18] supporting the DS picture of confinement in the context of supersymmetric  $N = 1$  gauge theories, we proposed an effective field theory (EFT) describing low energy physics for 4D  $U(1)$ lgt in terms of monopole fields [19]. The EFT should work regardless of the action chosen on the lattice provided the correlation length is sufficiently large.

In a later work, we tried to compare the predictions of the spectrum extracted from the EFT with the ones available from lattice simulations. This revealed some inconsistencies in lattice spectra [20]. Relying on a theorem in [21] we tried to match the results of [16] with the ones of [22, 23] (in the latter case the comparison can only be qualitative as these results are obtained with Villain action). This theorem states that, in the confined phase of 4D  $U(1)$ lgt, the Hilbert space of magnetically charged particles is contained into the Hilbert space of the neutral ones. Masses extracted from operators creating states with the same quantum numbers (angular momentum, parity and charge

conjugation ( $J^{PC}$ ) but with different magnetic charges should coincide. The monopole mass of [16] should coincide with the  $0^{++}$  gaugeball mass of [22] and the dual photon mass of [16] should coincide with the  $1^{-+}$  gaugeball mass of [22].

This, as we already pointed out [20], was clearly not the case even at a qualitative level. In [16], the monopole was heavier than the dual photon whereas in [22, 23] the scalar gaugeball was lighter than the axial vector gaugeball.

Later on, new results were obtained for the dual photon mass studying the electric flux tube profile between static charges [24, 25]. The results presented therein (assuming the dual superconductor picture) reconcile the dual photon mass with the one of the axial vector gaugeball. The only piece of the spectrum in disagreement with the theorem was the monopole mass as calculated in [16].

Our main result is to reconcile the value of the mass extracted from monopole correlators with the one of the  $0^{++}$  gaugeball.

For that purpose, we introduce a modified order parameter as explained in the next section. Then, we present the detailed analysis of data obtained simulating this new order parameter on the lattice. We check that a single particle is responsible for the decay of its two-point correlation function. We extract the mass of this particle and find complete agreement with that of the  $0^{++}$  gaugeball. Our method allows to extract a very good signal to noise ratio for the masses with an amount of data one order of magnitude smaller than that needed for existing techniques. We conclude with a discussion of the physical scenario emerging from our study.

### THE OPERATOR FOR SPECTRAL STUDIES

The partition function of 4D  $U(1)$ lgt is defined as:

$$Z(\beta) = \int \left( \prod_{(\vec{n}, t)} \prod_{\mu=0}^3 \mathcal{D}\theta_{\mu}(\vec{n}, t) \right) \exp(-\beta S).$$

We chose to consider the Wilson action:

$$S = - \sum_{(\vec{n}, t)} \sum_{i>\mu=0}^3 (\cos d\theta_{i\mu}(\vec{n}, t) - 1). \quad (1)$$

where  $\theta_{\mu}(\vec{n}, t)$  are the link variables of the four dimensional lattice whose sites are labelled by  $(\vec{n}, t)$ . We use  $i$  as index for spatial directions and  $\mu$  as index that spans all the four directions of the lattice. The field  $\theta_{\mu}(\vec{n}, t)$  take value in  $U(1)$  and  $\prod_{(\vec{n}, t)} \prod_{\mu=0}^3 \mathcal{D}\theta_{\mu}(\vec{n}, t)$  is the Lesbegue measure for each variable. We will abbreviate it as  $(\prod \mathcal{D}\theta)$ .  $d\theta_{i\mu}(\vec{n}, t)$  is the lattice field strength term obtained acting with the exterior derivative on the link variables.  $d\theta_{i\mu}(\vec{n}, t)$  is hence defined on plaquettes identified by the coordinates  $(\vec{n}, t)$  lying on the plane  $i - \mu$ . At last,  $\beta = \frac{1}{g^2}$  with  $g$  being the  $U(1)$  the coupling constant.

The order parameter for the Coulomb-Confined transition we consider was introduced by the Pisa group [15, 16]. It is the mean value of a monopole creation operator and shifts the plaquette field strength at a given Euclidean time by the contribution of the vector potential produced by a static magnetic source  $\vec{b}(\vec{x})$ . In the continuum, using standard notation this would be:

$$\mu(\vec{y}, t) |\vec{A}(\vec{x}, t)\rangle \equiv |\vec{A}(\vec{x}, t) + \frac{1}{e} \vec{b}(\vec{x} - \vec{y})\rangle \quad (2)$$

with

$$\mu(\vec{y}, t) = \exp \left[ i \frac{1}{e} \int d^3x \vec{E}(\vec{x}, t) \vec{b}(\vec{x} - \vec{y}) \right]. \quad (3)$$

Further details on the subject can be found directly in [16].

The lattice version of the operator is defined as:

$$\mu(\vec{y}, t) = \exp \sum_{\vec{n}} \sum_{i=1}^3 \beta (\cos(b_i(\vec{y} - \vec{n}) - d\theta_{i0}(\vec{n}, t)) - \cos(d\theta_{i0}(\vec{n}, t))) \quad (4)$$

If we consider the effect of a monopole antimonopole pair placed at points  $(\vec{x}, t_1)$  and  $(\vec{y}, t_2)$  on the lattice the corresponding correlator will be :

$$\begin{aligned} \langle \mu(\vec{x}, t_1) \bar{\mu}(\vec{y}, t_2) \rangle &= \frac{1}{Z} \int \left( \prod \mathcal{D}\theta \right) \prod_{(\vec{n}, t)} \prod_{i > \mu=1}^3 \exp \beta (\cos d\theta_{i\mu}(\vec{n}, t) - 1) \\ &\quad \prod_{\vec{n}, t \notin \{t_1, t_2\}} \prod_{i=1}^3 \exp \beta (\cos d\theta_{i0}(\vec{n}, t) - 1) \\ &\quad \prod_{\vec{n}, t \in \{t_1, t_2\}} \prod_{i=1}^3 \exp \beta (\cos(b_i(\vec{x}, \vec{y}, \vec{n}) - d\theta_{i0}(\vec{n}, t)) - 1). \end{aligned} \quad (5)$$

In this formula  $b_i(\vec{x}, \vec{y}, \vec{n}) = b_i(\vec{x} - \vec{n})_{t=t_1} - b_i(\vec{y} - \vec{n})_{t=t_2}$  is the  $i$  component of the lattice vector potential produced by the monopole anti-monopole pair. It has support only on the two time slices  $t_1$  and  $t_2$ . From now on we will consider the case for which  $\vec{x} = \vec{y}$  and the external field will be denoted  $b_i(\vec{x} - \vec{n})$ .

The expectation value (4) is very difficult to extract from Monte-Carlo simulations. In order to see why this is so we define a new operator

$$\mathcal{O}(\Delta t) = \prod_{\vec{n}, t \in \{t_1, t_2\}} \prod_{i=1}^3 \exp \beta (\cos(b_i(\vec{x} - \vec{n}) - d\theta_{i0}(\vec{n}, t)) - 1) \quad (6)$$

where, to simplify the notation, we have ignored its dependency on all variables but  $\Delta t = |t_2 - t_1|$ . This is justified by the fact that we will always deal with expectation values of (6) that really depends (among other variables) on  $\Delta t$ . We introduce a modified action:

$$\tilde{S} = - \sum_{(\vec{n}, t)} \sum_{i > \mu=1}^3 (\cos d\theta_{i\mu}(\vec{n}, t) - 1) - \sum_{\vec{n}, t \notin \{t_1, t_2\}} \sum_{i=1}^3 (\cos d\theta_{i0}(\vec{n}, t) - 1). \quad (7)$$

It is important to notice that the action (7) differs from the standard action (1) only on the two time-slices  $t_1$  and  $t_2$  where the monopole operator has support. On these time-slices (7) vanishes.

We can express the two point correlation function (5) as the mean value of the operator (6) on configurations generated with (7):

$$\langle \mu(\vec{x}, t_1) \bar{\mu}(\vec{x}, t_2) \rangle = \frac{1}{Z} \int \left( \prod \mathcal{D}\theta \right) \exp \left( -\beta \tilde{S} \right) \mathcal{O}(\Delta t) \quad (8)$$

In this way the difficulty in measuring (5) appears immediately: we are trying to extract the mean value of (6) on configurations sampled uniformly on its support. On the time-slice  $t_1$  and  $t_2$ , support of (6), the term  $-\cos(d\theta_{i0}(\vec{n}, t))$  coming from (4) cancels the analog contribution coming from the action (1). In this way, on these time slices, importance sampling is lost.

This is one of the reasons that forced the authors of [16] to introduce:

$$\rho = - \frac{\partial}{\partial \beta} \log \langle \mu(\vec{x}, t_1) \bar{\mu}(\vec{y}, t_2) \rangle \quad (9)$$

With this definition one recovers the importance sampling on the time-slices  $t_1$  and  $t_2$ . On them the action becomes:

$$S'(t_1, t_2) = \sum_{\vec{n}, t \in \{t_1, t_2\}} \sum_{i=1}^3 \cos(b_i(\vec{x} - \vec{n}) - d\theta_{i0}(\vec{n}, t)) - 1 \quad (10)$$

If one is interested in studying the mean value of  $\rho$  this is enough [16]. In our case we need to go a little further as we want to extract masses in the confined phase. To do this we are forced to study the decay of (5) as function of the time separation  $t$  between monopole and antimonopole. Assuming that for large  $t$  the decay of (5) is driven by a single particle, in the confined phase, we obtain:

$$\langle \mu(\vec{x}, t) \bar{\mu}(\vec{x}, 0) \rangle \sim \mu^2 + AM^{1/2} t^{-3/2} e^{-Mt}. \quad (11)$$

In this formula  $\mu$  is the v.e.v of the monopole operator  $\mu(\vec{x}, t)$ . It is different from zero in the confined phase.  $A$  is the projection of the monopole state on the vacuum.  $M$  is the monopole mass. In order to keep formulas compact we are neglecting the effect of periodic boundary conditions but we will add them when studying numerical results.

Fluctuations of (9), in the confined phase, are caused by fluctuation of the v.e.v.  $\mu^2$  and completely screen the decay (11) we need to unmask to extract  $M$ . To deal with this in [16] a very huge amount of data was collected. We can, however, introduce a new definition of  $\rho$  that, following the ideas introduced in [22] in the context of gaugeball spectroscopy, approximates the connected part of (5) and eliminates  $\mu^2$ . The new operator is defined as:

$$\rho' = \frac{\partial}{\partial t} \log \langle \mu(\vec{x}, t) \bar{\mu}(\vec{x}, 0) \rangle. \quad (12)$$

With this definition importance sampling on the monopole anti-monopole time slices is kept (as in the case of (9)) and fluctuations at  $\mu^2$  scale are eliminated. Starting from (11) we obtain the large  $t$  behaviour of (12):

$$\rho' \sim AM^{1/2} t^{-3/2} e^{-Mt} \left( -M - \frac{3}{2t} \right) \left( \mu^2 + AM^{1/2} t^{-3/2} e^{-Mt} \right)^{-1} \quad (13)$$

This expression has 3 free parameters:  $\mu, M, A$ . On a large enough lattice we can expand (13) in a regime where  $\mu^2 \gg AM^{1/2} t^{-3/2} e^{-Mt}$ . At first order in  $\frac{AM^{1/2}}{\mu^2} t^{-3/2} e^{-Mt}$  we get from (13):

$$\rho' \sim \left( -M - \frac{3}{2t} \right) \frac{AM^{1/2}}{\mu^2} t^{-3/2} e^{-Mt}$$

from which it is easier to extract a precise determination of the mass. However the results presented in this paper are obtained with the full expression (13).

The simulation algorithm for studying  $\rho'$  decays is very similar to the one needed to study  $\rho$  decays. Starting from the expression (8) and taking the logarithm we get

$$\partial_t \log \langle \mu(\vec{x}, t) \bar{\mu}(\vec{x}, 0) \rangle = \frac{\int (\prod \mathcal{D}\theta) \exp(-\beta \tilde{S}) \partial_t \mathcal{O}(t)}{\int (\prod \mathcal{D}\theta) \exp(-\beta \tilde{S}) \mathcal{O}(t_0)} \quad (14)$$

We need to use the first order approximation in  $\partial_t f$ :

$$\partial_t e^{f(t)}|_{t=t_0} = e^{f(t)} (\partial_t f)|_{t=t_0} \quad (15)$$

In this way we can express the derivative as :

$$\partial_t \mathcal{O}(t) = \mathcal{O}(t) \sum_{\vec{n}} \sum_{i=1}^3 \partial_t (\beta (\cos(b_i(\vec{n})) - d\theta_{i0}(\vec{n}, t_0)) - 1)$$

and we can include the factor  $\mathcal{O}(t)$  in the measure. This defines a new action:

$$S' = \tilde{S} + \sum_{\vec{n}} \sum_{i=1}^3 \cos(b_i(\vec{n})) - d\theta_{i0}(\vec{n}, t) - 1.$$

The expression (14) in this way becomes:

$$\partial_t \log \langle \mu(\vec{x}, t) \bar{\mu}(\vec{x}, 0) \rangle = \frac{1}{Z'} \int \left( \prod \mathcal{D}\theta \right) e^{-\beta S'} \partial_t (\log \mathcal{O}(t) - \beta S(t)). \quad (16)$$

where  $S(t)$  is the Wilson action defined in (1) restricted on the time slices  $t$  and 0. We hence need to compute the mean value of

$$\partial_t (\log \mathcal{O}(t) - \beta S(t))$$

on configurations generated with  $S'$ :

$$\rho' = \langle \partial_t (\log \mathcal{O}(t) - \beta S(t)) \rangle' \quad (17)$$

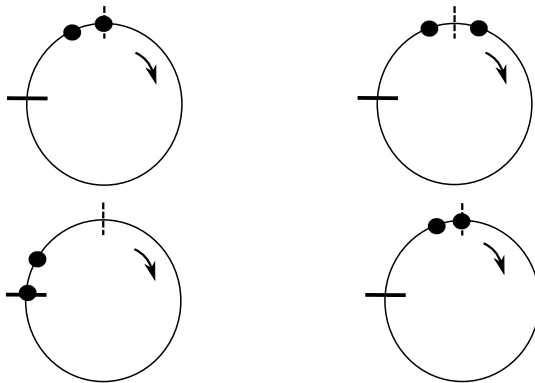


FIG. 1: This figure represents the configurations we used to calculate the discrete derivative. The circle represents the time direction of our lattice. The thick lines represent monopole and anti-monopole terms included in the action. The solid points represent the time slices used to measure the operator and construct the derivatives. On the left hand side we see the symmetries of the construction when interchanging monopole and anti-monopole derivatives. On the right hand side differences between symmetric and backward derivatives are sketched.

To calculate the derivative of  $\log \mathcal{O}(t) - \beta S(t)$  numerically in principle we could choose the forward, backward or symmetric prescriptions. We are considering, however, the approximation (15) with  $f(t) = \partial_t (\log \mathcal{O}(t) - S(t))$  and hence need to minimize  $f(t)$ . This requirement immediately selects the symmetric prescription  $f'(t) = (f(t+1) - f(t-1))/2$ . The reason for that is outlined in the right part of figure 1. There, we sketch the scenario used in our computations. The circle represents the temporal direction of the lattice (the other directions are omitted for simplicity) and the dashed and solid thick lines represent the insertion of monopole and anti-monopole operators in the action (10) at the two time slices separated by a distance  $t$ . The solid dots represent the time slices used to calculate the derivative in the symmetric case and in the backward case. Symmetric derivatives involve time slices separated by two lattice spacings. Nevertheless, their plaquettes are updated with the same action and are hence more correlated than the adjacent time slices involved in the backward or forward derivatives calculations. These last are updated with different actions since on one of them there is the monopole (or anti-monopole) contribution. The symmetric prescription, hence, minimizes  $\partial_t (\log \mathcal{O}(t) - S(t))$  and is used to extract the correct value of  $\rho'$ .

In order to obtain (12) from (5) we have a further freedom: we can derive the correlator either with respect to the monopole or to the anti-monopole position, the only difference being an overall minus sign. This is shown on the left part of figure 1. Derivatives on the monopole field amount to minus derivatives on the anti-monopole field.

## NUMERICAL RESULTS

We performed three runs of simulations on three different lattices. The smallest is a  $6^3 \times 12$  lattice the medium is a  $8^3 \times 16$  and the largest  $10^3 \times 20$ . We collected over 400000 sweeps of statistics for all the lattices. We used the standard 1 heat-bath and 3 over-relaxation algorithm. In order to extract the value of the masses from the numerical data, we have to include the effect of periodic boundary conditions (p.b.c.). Once we define  $f(x) = AM^{1/2}x^{-3/2}e^{-Mx}$ , the p.b.c. modify (11) producing:

$$\langle \mu(\vec{x}, t_1) \bar{\mu}(\vec{x}, t_2) \rangle \sim \mu^2 + f(r) + f(r_t) + 3(f(r_s) + f(r_{st}) + f(r_{ss}) + f(r_{sst})). \quad (18)$$

where  $r_t, r_s, r_{ss}$  take into account the different path we can choose to go from  $(\vec{x}, t_1)$  to  $(\vec{x}, t_2)$ . We can in fact choose the shortest path ( $r = t = |t_2 - t_1|$ ) or the path that winds once in the temporal direction ( $r_t = L - t$ ); we can also wind once around the spatial direction ( $r_s = \sqrt{t^2 + L_s^2}$ , we have three different choices), twice around the spatial direction ( $r_{ss} = \sqrt{t^2 + (2L_s)^2}$  we have three possible choices) once around the spatial and the time direction ( $r_{st} = \sqrt{(L-t)^2 + L_s^2}$  we have three possible choices) and twice around the spatial direction and one around the time direction ( $r_{sst} = \sqrt{(L-t)^2 + (2L_s)^2}$  we have three possible choices). Taking into account all these possibilities we extracted the masses depicted in figure 3 in a range of  $\beta$  which ensured the system is in the confined phase. The first thing we notice from figure 2 is that, for all the values of  $\beta$  considered, the  $\chi^2/n.d.f.$  obtained fitting the numerical data with expression (13) is lower than one. The only exceptions are, indeed, points very close to the transition

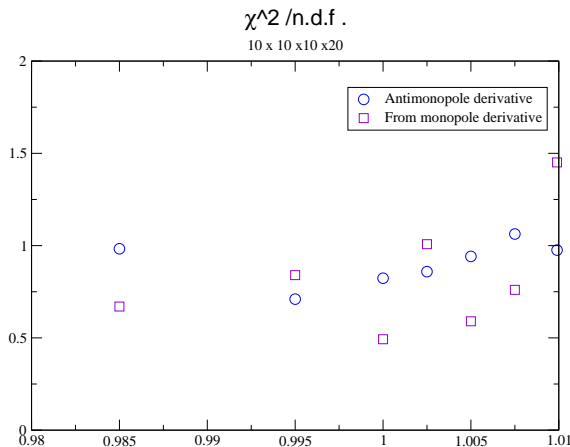


FIG. 2: This figure is a plot of the  $\chi^2/n.d.f.$  for the fits we performed with expression (13) on the lattice  $10^3 \times 20$ . For each  $\beta$  we have at least one channel with  $\chi^2/n.d.f. \ll 1$ . This confirms the validity of (13) to describe the correlator decay.

(which is first order with very long correlation length) and are surely due to metastabilities caused by our updating algorithm. This means that the leading contribution to the decay is correctly described by a single particle excitation. As explained in the previous section, we use the symmetric prescription for the derivative in expression (17) and derive both with respect to the monopole and anti-monopole position. From the figure 3 it is clear that the masses extracted in both cases are compatible within error-bars.

In figure 4 we show typical data-points we obtain for the derivative of the correlation function (17) from the simulations performed. The line represents the best-fit curve. The upper plot contains points obtained deriving with respect to the monopole position whether the lower plot contains points obtained deriving with respect to the antimonopole position. In both cases we were forced to add a constant term to the expression (13) to correct from systematic errors induced by discretization and by expanding the exponential of the derivative in (15). The best-fit curves are obtained using a subset of distances (from 4 to 16) to avoid contamination from higher states in the same channel and safely consider only the single particle decay.

Comparing our results with the ones in [16] one notices a clear improvement of the signal to noise ratio. The difference between the values of the masses we extract and the ones obtained in [16] is probably due to the high noise that prevented the authors of [16] from using the full expression (18) in fits. The authors, forced to use a zero momentum approximation of the decay (11), introduced a systematic error that shifted the masses from their actual value.

We can also safely identify the particle responsible for the decay. The masses we get from the fit with the complete expression (18) are indeed fully compatible with the known value for the gaugeball  $0^{++}$  mass (see i.e. [22] for a recent high precision study). To show this we took into account finite size effects in the two plots 5.

In the first we considered the results we obtained for the masses (from both monopole and anti-monopole channels) at  $\beta = 1.005$ . We plotted them versus the lattice size (calculated as  $L = (L_s^3 \times L_t)^{1/4}$ ). The last point at  $L = 16$  is taken from the results of the  $0^{++}$  mass contained in [22]. Under the assumption that the discrepancy between our results and the one [22] is due to finite size effects we made a two parameters fit with the expression  $M(L) = M_\infty - AL^{-1}$ . In the second plot there is the same study at  $\beta = 1.0099$ . The  $\chi^2$  values safely confirm the identification of the particle responsible for the decay (11) with the  $0^{++}$  gaugeball. Furthermore the fact that the thermodynamic limit is approached from below is the expected behaviour in the confined phase (see i.e. [26]). These results confirm the validity of a theorem about the structure of the Hilbert space in the confined phase of compact lattice  $U(1)$  in four dimensions proved in [21]: there are no super-selected sectors labelled by the magnetic charge. The last point to stress is that our method prevents a precise measurement of the v.e.v.  $\mu$  (as it is designed to get rid of it as far as possible). This is shown in figure 6 and implies that, if interested in studying the order parameter for the Coulomb Confined transition, one should better use the standard  $\rho$  definition [15].

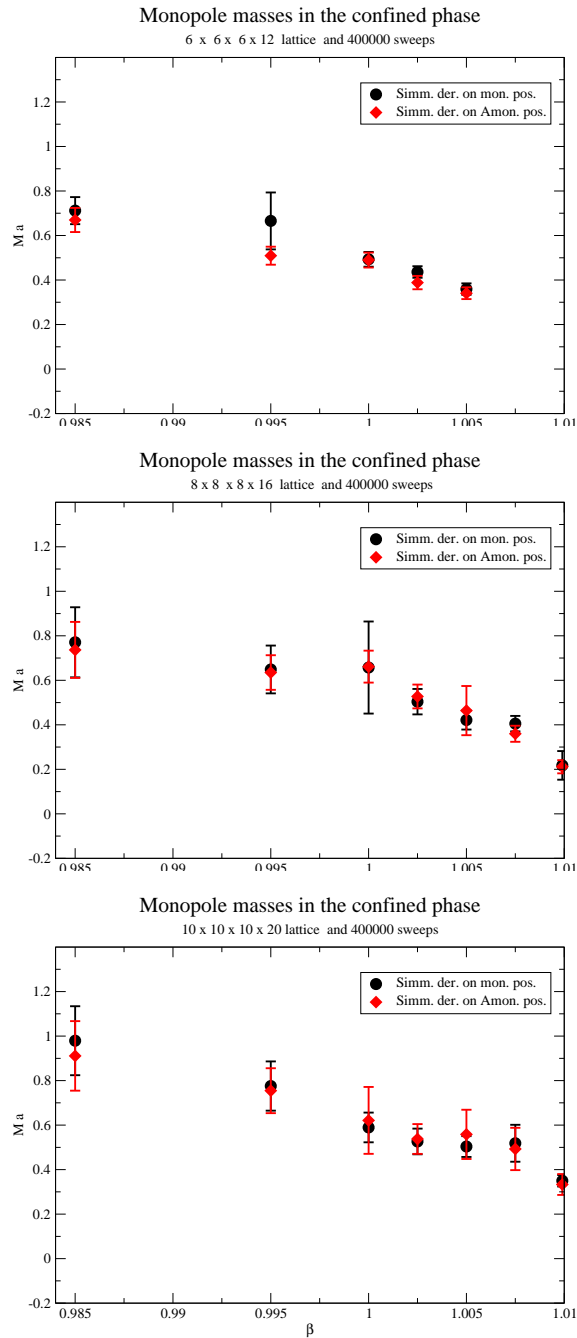


FIG. 3: These figures collect masses calculated with the two possible strategies on the three lattice sizes we considered in a range of  $\beta$  in the confined phase. We can derive the correlation function either with respect to the monopole position or to the anti-monopole position. Masses extracted with any of these prescriptions are compatible within error bars.

## CONCLUSIONS

In this work we considered the spectrum extracted from magnetically charged operators. We introduced a new powerful technique that reduces, with respect to existing methods, one order of magnitude the amount of data necessary to extract a good signal for correlations of such operators.

The improvement of the technique relies on the fact that it allows to study the connected part of the correlation functions. As a first application we study the Hilbert space of confined compact four dimensional  $U(1)$  theory. We consider monopole anti-monopole correlation functions on three lattice sizes ( $6^3 \times 12$ ,  $8^3 \times 16$ ,  $10^3 \times 20$ ). We check

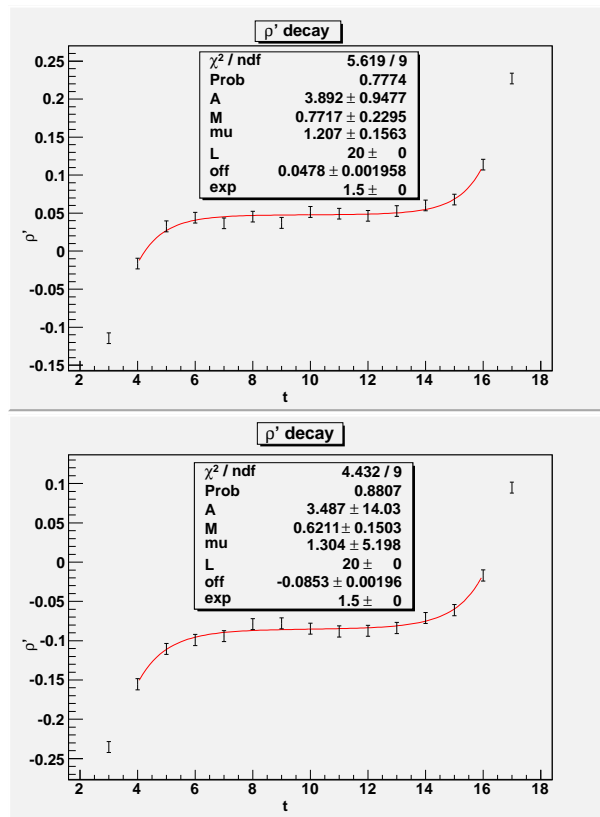


FIG. 4: This figure represents the correlation function decay for a  $10^3 \times 20$  lattice at  $\beta = 1$ . The points on the upper plot are obtained deriving with respect to the monopole field, while the point on the lower part deriving with respect to the anti-monopole field .

that the large time correlation functions decay is driven by a single particle. We also identify this particle by studying its mass. The value for the mass we extract is compatible with the one found in literature for the gaugeball  $0^{++}$ . This is in complete agreement with a theorem proved in [21] stating that the Hilbert space of compact lattice  $U(1)$  in four dimensions does not contains any magnetically super-selected sectors. Completing our results with the ones obtained by other groups with different techniques [22, 24, 25] one can have a full picture of the Hilbert space of compact  $U(1)$  lattice gauge theory in four dimensions as the space spanned by gaugeball states. We are working on similar studies for the case of non Abelian lattice gauge theories. We are also working on the implementation of a new algorithm to measure directly the order parameter  $\vec{\mu}(\vec{x}, t)$  and its finite size scaling based on ideas similar to the ones presented in this work.

## ACKNOWLEDGEMENTS

The work was partially financed by a graduate scholarship of the Spanish M.E.C. I would like to acknowledge D. Espriu, A. Di Giacomo, F. Gliozzi, G. Paffuti and C. Pica for the precious discussions and suggestions on the topics covered by this work. I also want to acknowledge M. D'Elia for correcting an error in a preliminary version of this work and the Physics Department at the Pisa University for its hospitality during the earlier stage of this work.

---

\* Electronic address: luca@ecm.ub.es

- [1] K. G. Wilson, Phys. Rev. **D10**, 2445 (1974).
- [2] R. Balian, J. M. Drouffe, and C. Itzykson, Phys. Rev. **D10**, 3376 (1974).
- [3] R. Balian, J. M. Drouffe, and C. Itzykson, Phys. Rev. **D11**, 2098 (1975).



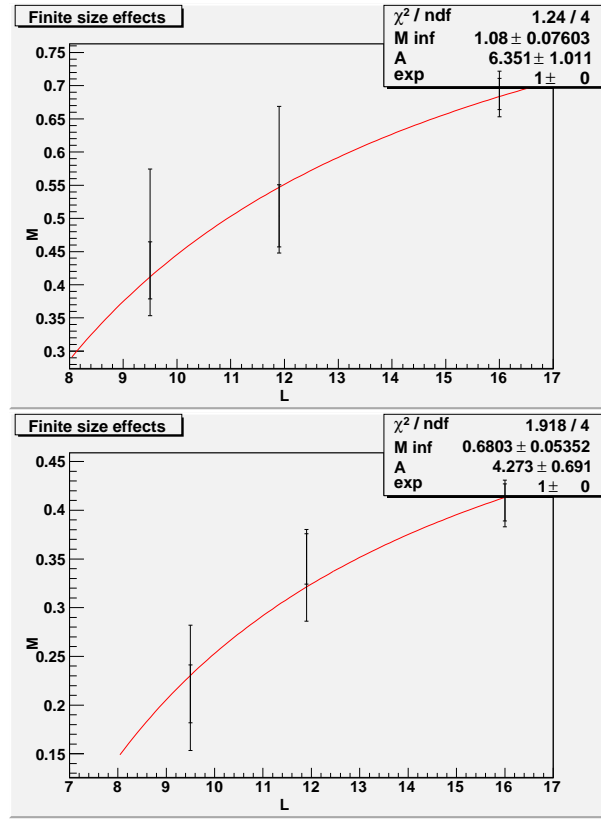


FIG. 5: These plots show the test of the assumption that the discrepancies between our results and the one contained in [22] for the  $0^{++}$  mass are finite size effects. We plot the mass against the linear size of the lattice for two different choices of  $\beta$  close to the transition. The last point in both plots (the one at  $L = 16$ ) is the  $0^{++}$  mass taken from [22]. The upper plot is at  $\beta = 1.005$ . The lower plot is at  $\beta = 1.0099$ . We considered only the two bigger lattices as for them the scaling should be dominated by  $1/L$  effects. We considered jointly results extracted from both monopole and antimonopole channels. The values of the  $\chi^2$  we obtain from the fit confirm the identification of the state we are studying with the  $0^{++}$  gaugeball.

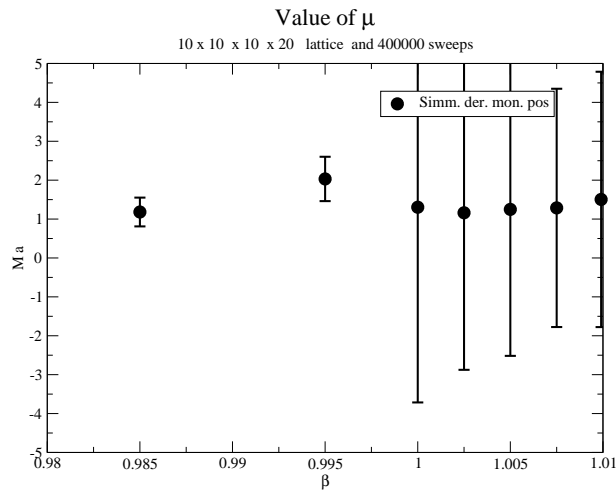


FIG. 6: V.e.v. of  $\mu$  extracted from our definition of  $\rho'$ . This plot shows that this operator is not adequate to measure the order parameter for the Coulomb-Confined transition.

- [4] M. Creutz, L. Jacobs, and C. Rebbi, Phys. Rev. **D20**, 1915 (1979).
- [5] B. Lautrup and M. Nauenberg, Phys. Lett. **B95**, 63 (1980).
- [6] H. G. Evertz, J. Jersak, T. Neuhaus, and P. M. Zerwas, Nucl. Phys. **B251**, 279 (1985).
- [7] G. Arnold, T. Lippert, K. Schilling, and T. Neuhaus, Nucl. Phys. Proc. Suppl. **94**, 651 (2001), hep-lat/0011058.
- [8] M. Vettorazzo and P. de Forcrand, Nucl. Phys. **B686**, 85 (2004), hep-lat/0311006.
- [9] A. M. Polyakov, Phys. Lett. **B59**, 82 (1975).
- [10] S. Mandelstam, Phys. Lett. **B53**, 476 (1975).
- [11] G. 't Hooft (1975), lectures given at Int. School of Subnuclear Physics, 'Ettore Majorana', Erice, Sicily, Jul 11-31.
- [12] T. A. DeGrand and D. Toussaint, Phys. Rev. **D22**, 2478 (1980).
- [13] J. Frohlich and P. A. Marchetti, Commun. Math. Phys. **112**, 343 (1987).
- [14] L. Polley and U. J. Wiese, Nucl. Phys. **B356**, 629 (1991).
- [15] L. Del Debbio, A. Di Giacomo, and G. Paffuti, Phys. Lett. **B349**, 513 (1995), hep-lat/9403013.
- [16] A. Di Giacomo and G. Paffuti, Phys. Rev. **D56**, 6816 (1997), hep-lat/9707003.
- [17] J. Jersak, T. Neuhaus, and H. Pfeiffer, Phys. Rev. **D60**, 054502 (1999), hep-lat/9903034.
- [18] N. Seiberg and E. Witten, Nucl. Phys. **B426**, 19 (1994), hep-th/9407087.
- [19] D. Espriu and L. Tagliacozzo, Phys. Lett. **B557**, 125 (2003), hep-th/0301086.
- [20] D. Espriu and L. Tagliacozzo, Phys. Lett. **B602**, 137 (2004), hep-th/0405015.
- [21] J. Frohlich and P. A. Marchetti, Europhys. Lett. **2**, 933 (1986).
- [22] P. Majumdar, Y. Koma, and M. Koma, Nucl. Phys. **B677**, 273 (2004), hep-lat/0309003.
- [23] J. Cox et al., Nucl. Phys. Proc. Suppl. **63**, 691 (1998), hep-lat/9709054.
- [24] M. Panero, JHEP **05**, 066 (2005), hep-lat/0503024.
- [25] Y. Koma, M. Koma, and P. Majumdar, Nucl. Phys. **B692**, 209 (2004), hep-lat/0311016.
- [26] I. Montvay and G. Munster (1994), cambridge, UK: Univ. Pr. 491 p. (Cambridge monographs on mathematical physics).